EFFECTS OF TEMPERATURE AND MOISTURE ON MODULE LEAKAGE CURRENTS*

G. Mon,** L. Wen,** R.G. Ross, Jr.,*** and D. Adent**

Jet Propulsion Laboratory - California Institute of Technology
Pasadena, California 91109

ABSTRACT

Module moisture level and operating temperature play a key role in determining the rate of many life-limiting processes such as corrosion, photothermal degradation of encapsulants, and voltage breakdown of module electrical insulation systems. An approach to mathematically simulating module leakage currents is presented and used to highlight the need for a detailed understanding of the moisture-sorption and transmission properties of the module, and the parametric dependence of leakage currents on the time-varying moisture and temperature level. Experimental and analytical results are presented that characterize the rate dependency of leakage currents on environmental temperature and humidity level and quantify the influence of module construction features such as rear-surface films and foils, cell-frame gap spacings, and encapsulant resistivity and thickness. The relative roles of surface and bulk resistivity are illuminated together with their differing dependencies on surface moisture, bulk moisture, and temperature.

INTRODUCTION

Two of the most fundamental parameters governing rate of degradation of photovoltaic modules are temperature and humidity. Most of the chemical reactions involved in degradation such as corrosion of cell metallizations and photodegradation of encapsulants have been found to be strong functions of these parameters (1,2,3,4). Temperature-rate relationships are generally found to be Arrhenius in character (log reaction rate inversely proportional to reciprocal absolute temperature) with a rate doubling for approximately every 10°C increase in temperature. Increased humidity also increases the reaction rate, but the mechanism is more complex and varied (5, 6). Although all parts of a PV module are approximately at the same temperature (±3°C), the moisture level in a module can vary by orders of magnitude from surface to module interior. This greatly complicates the computation of moisture effects because the moisture level must be specifically computed for the exact site of the governing reaction, be it cell-encapsulant interface or module exterior surface. Quantifying the reaction rates expected under varying field conditions requires complex transient models of the modules' spatial moisture sorption together with detailed knowledge of the reaction-rate dependency on this moisture level and distribution.

This paper explores the role of temperature and humidity in controlling module electrical leakage currents and presents experimental and analytical results detailing the complicating influences of module construction features such as rear-surface films and foils, cell-frame gap spacings, and encapsulant resistivity and thickness. Special attention is given the differing roles of surface and bulk conductivity as separately influenced by surface and bulk moisture levels.

Background

When a photovoltaic module is mounted in a field application, its solar cells will operate at a voltage relative to ground determined by the module's position in the overall array circuit. For a large high-voltage central-station with center-tapped array, the cells may be as much as 500 volts positive or negative with respect to ground, i.e., with respect to the module's frame. This cell-frame voltage gradient gives rise to low-level leakage currents between cell and frame, which over prolonged periods can cause electrochemical corrosion of the module metallic components (1,2).

The leakage current is composed of charge carriers (ions) that move under the influence of the voltage and concentration gradients through the insulation, reacting with it and with the cell and frame metals to produce corrosion products.

---

*This paper presents the results of one phase of research conducted at the Jet Propulsion Laboratory, California Institute of Technology, for the U.S. Department of Energy, through an agreement with the National Aeronautics and Space Administration.

**Member of the Technical Staff, Reliability and Engineering Sciences Area, Flat-Plate Solar Array Project, System Integration Section.

***Reliability and Engineering Sciences Manager, Flat-Plate Solar Array Project, and Supervisor, Photovoltaic Engineering Group, System Integration Section.

Proceedings of the 18th IEEE Photovoltaic Specialists Conference
Las Vegas, Nevada, October 21-25, 1985, pp. 1179-1185.

With positive polarity (cell positive relative to the frame), corrosion is characterized by loss of cell metallization and the formation of cathodic dendrites; the dissolved cell metallization ions migrate to the frame, upon which they deposit as dendritic crystallites. The metallization ions also react with the encapsulant, clouding and discoloring it.

Typical corrosion with negative polarity exhibits less obvious characteristics to the naked eye, but microscopic examination reveals the formation of anodic corrosion salts and the evolution of gas bubbles at the cell's metallization-silicon interface. This results in metallization delamination and consequently increased cell series resistance.

The rate at which these reactions occur is proportional to the leakage current level as determined in large part by the electrical ionic conductivity of the insulation; this conductivity varies greatly with temperature and relative humidity as indicated for two popular photovoltaic insulations in Figure 1 (1). Note that for the same conditions of temperature and humidity, the bulk conductivity of polyvinyl butyral (PVB) is about three orders of magnitude larger than that of ethylene vinyl acetate (EVA).

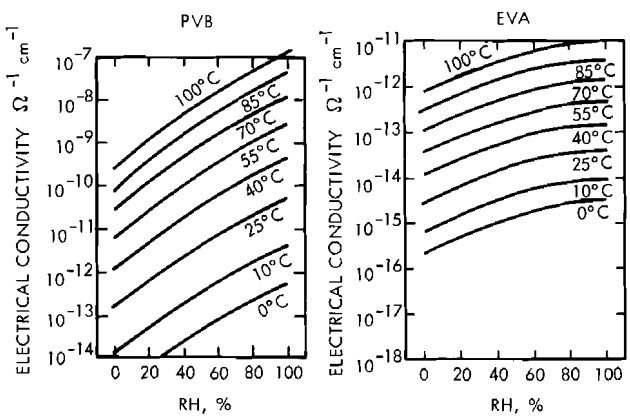

Figure 1. Bulk Electrical Conductivity of PVB and EVA

Leakage current integrated over time yields charge transferred between the cell and the frame. The quantity of charge transferred is an important measure of the total degree of electrochemical corrosion and the resulting damage, such as cell power output reduction. Previous studies have quantified this relationship for crystalline and amorphous-silicon modules and have shown that 0.1 to 1 C/cm (α-Si) and 1 to 10 C/cm (C-Si) of charge transferred between cell and frame are required to produce a significant level, approximately 50%, of cell failures (1,2,7). The assumption that equal quantities of charge transferred in laboratory and field environments produce equivalent electrochemical damage, is the fundamental premise behind electrochemical-corrosion life prediction (1). The overall process of life simulation, as currently implemented at JPL, is schematically illustrated in Figure 2. Research is underway to generate the characterizations associated with the heavy-lined boxes in this figure. The focus of this paper is the temperature-moisture resistivity correlation and computation of leakage current levels as a function of temperature, humidity, and module configuration.

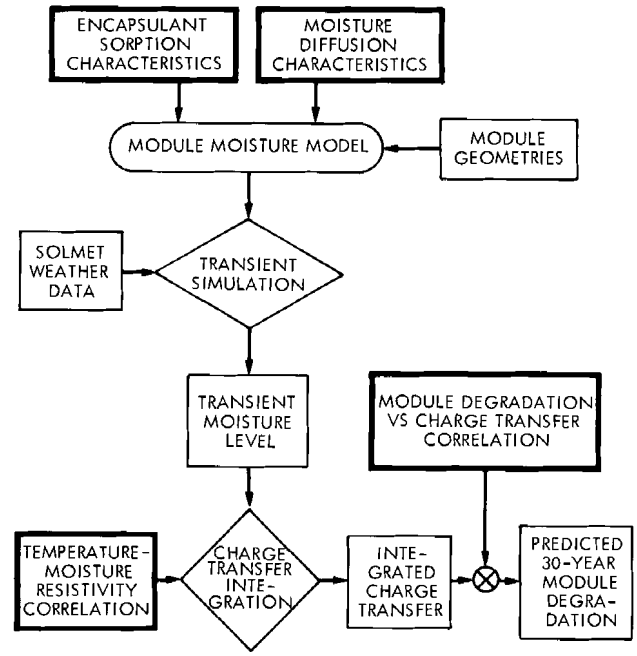

Figure 2. Photovoltaic Module Life Prediction

In preliminary life-simulation analyses by these authors (1,2) simplified assumptions were made to allow path-finder field-test correlations to be estimated. These assumptions included:

(1) The entire module encapsulant is always in instantaneous equilibrium with the external temperature-humidity environment.

(2) The leakage current is proportional to the bulk conductivity of the module encapsulant as determined by the instantaneous T and RH level; the conductivity of the encapsulant was assumed to be unaffected by the level of accrued corrosion.

(3) The leakage current of foil-backed modules is determined by the encapsulant's temperature dependency only; the as-laminated level of humidity in foil-backed modules was assumed near zero due to the vacuum lamination process.

EXPERIMENTAL STUDY OF LEAKAGE CURRENTS (XTEST)

To help quantify the true dependency of leakage currents on temperature, humidity, and the many module design parameters, an extensive parametric test program referred to in-house as XTEST, has recently been completed. In this

experiment a number of module-like test samples was fabricated using crystalline-silicon solar cells and aluminum frame electrodes as shown in Figure 3. To provide a known electrochemical environment each cell-frame combination was laminated to a 10-cm by 13-cm glass sheet using a variety of encapsulation systems based on the well-characterized encapsulants PVB and EVA. The key design parameters were (1) encapsulations: PVB and EVA; (2) back surface films: none (bare), polymer (Tedlar), and polymer/metal composite film (Tedlar/Polyester/Aluminum/Tedlar, TPAT); (3) cell-frame electrode spacing: 0.13 cm and 1.3 cm, nominal; and (4) electrical polarity: 500 volts positive and negative, and unelectrified (controls). These parameter combinations required 24 electrified samples.

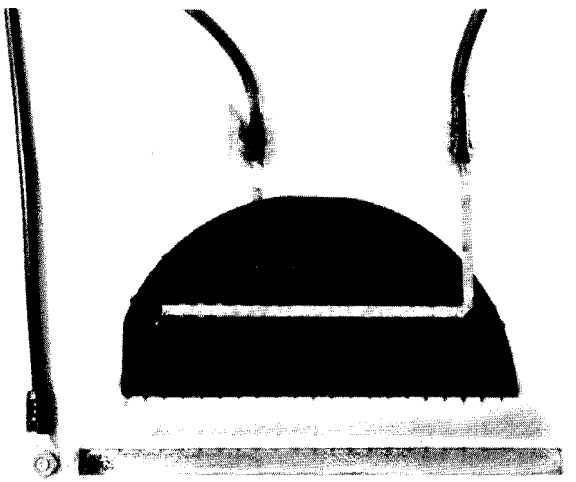

Figure 3. Typical XTEST Test Sample

Two identical Blue-M controlled temperature-humidity chambers were used to expose the samples to a stepped sequence of up to 6 increasing, then decreasing, relative humidities at each of four constant temperatures: 40°C, 55°C, 70°C and 85°C. The computer-controlled data acquisition system obtained leakage current measurements every 30 minutes during sample exposure, and cell I-V performance was measured after each constant temperature run.

Each of the environmental test levels was held until equilibrium was reached, often requiring as much as 100 hours per level. The total exposure required approximately 3000 hours of testing. After completion of the entire environmental sequence a number of the early data points were repeated to assess the effect of the accrued corrosion on the initial leakage-current levels.

Figure 4 shows the measured leakage current variation with time for a representative data sequence. Because of the constant-environment nature of the temperature-humidity chamber, it is possible to extract approximate time constants from the step-response data as shown. Although a great deal of variability was noted, humidity time constants generally ranged from a few hours to as much as 30 hours for all-polymeric samples. Because of slow leakage around the edges of the foil samples, they exhibited very long time constants (hundreds of hours) and surely never reached their true long-term equilibriums. The conclusion that must be drawn is that instantaneous equilibrium is a poor assumption for any of the samples when computing leakage current responses to diurnal humidity changes.

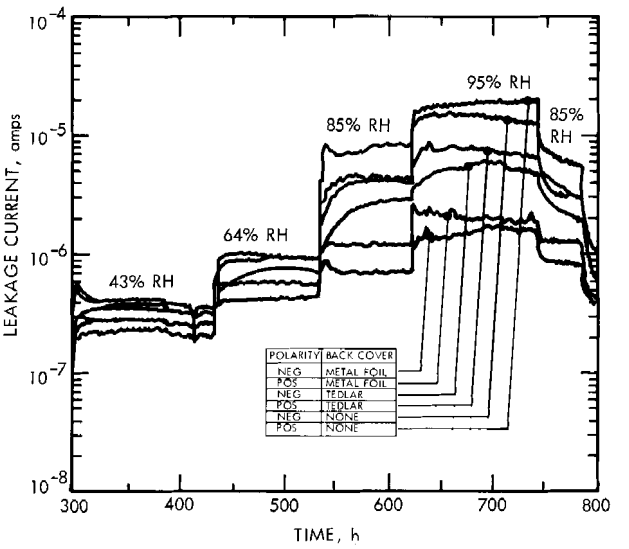

Figure 4. Typical Leakage-Current-versus-Time Data

Test Results

A global least squares curve fitting technique, used originally to fit a second degree polynomial to the bulk PVB and EVA conductivity data in Figure 1, was used to generate equilibrium leakage current versus relative humidity isotherms for each test specimen. A complete set of isotherms is presented in Figures 5 and 6, for PVB and EVA samples, respectively, with positive polarity; because no statistical difference was found in the data obtained using 0.13 cm versus 1.3 cm cell-frame gap spacings, the data for the two spacings were combined in the above figures.

A number of observations can be drawn from the XTEST results and are described below:

Polarity of Applied Voltage. For all samples, leakage current magnitudes in negative polarity were less than those in positive polarity by about a factor of 2 (e.g., see Figure 4). This difference seems to be associated with the ease of ionization of the ion donor (positive) electrode. The current is larger when this anode is the silver cell metallization, and lower when the anode is the aluminum frame member. Other cell metallizations have been found to have similar influences on the leakage-current levels. For example, Nickel-solder systems have lower leakage-current rates like those with the aluminum electrodes

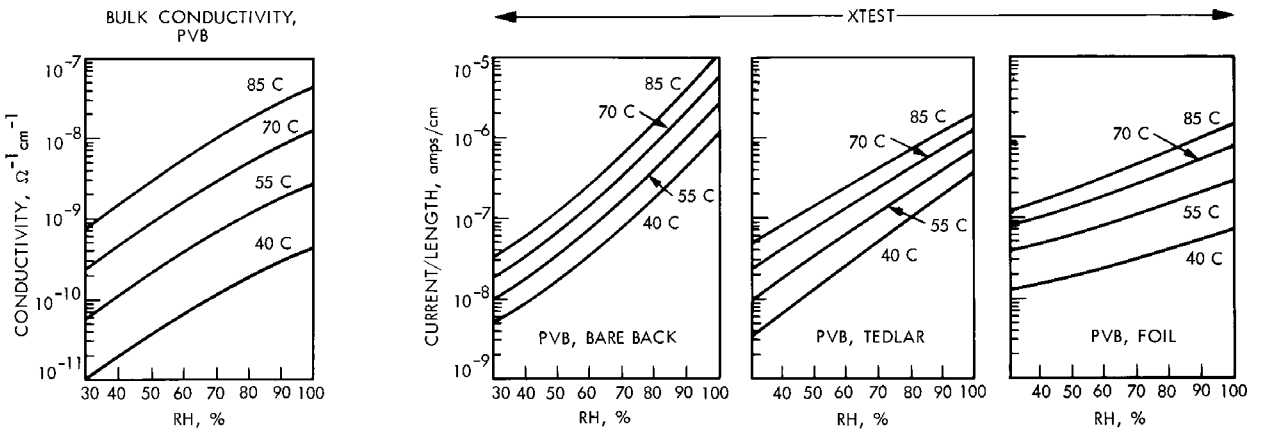

Figure 5. Leakage Current versus Temperature and Relative Humidity for Positive Polarity PVB XTEST Samples, and Bulk Conductivity of PVB

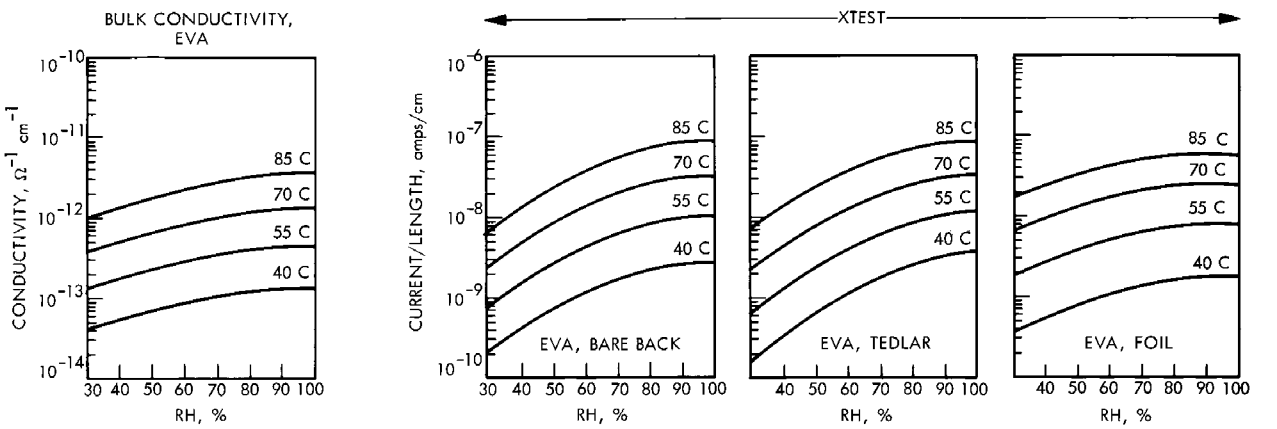

Figure 6. Leakage Current versus Temperature and Relative Humidity for Positive Polarity EVA XTEST Samples, and Bulk Conductivity of EVA

(1). Because of the similarity of the results with the two polarities, the discussions that follow are applicable to either.

Sensitivity to Temperature. In previous simulation studies (1) it was assumed that the temperature sensitivity of the module leakage current matched that of the encapsulant bulk conductivity as shown in Figure 1. By including all the synergistic elements of a complete module, the XTEST specimens provided a rigorous test of this assumption. Because many rate-dependencies on temperature follow an Arrhenius relationship, with a rate doubling for approximately every 10°C, it is useful to characterize the temperature sensitivities contained in Figures 5 and 6 in terms of fractional leakage-current increase per 10°C; this is displayed in Table 1. From these data it is clear that the factor-of-2-per-10°C rule of thumb is excellent for the EVA samples, which display identical sensitivity to that of the bulk EVA. On the other hand, the PVB samples display a somewhat lower sensitivity (1.5 to 1.8 per 10°C), which is significantly less than the high (2.7 per 10°C) temperature sensitivity of the bulk PVB. This implies that there is a dominant resistance, in addition to the PVB itself, and this additional

Table 1. Temperature Sensitivity of Leakage Current (Factor Increase per 10°C)

Sample Configuration	Humidity Level: Low (30-50% RH)	Humidity Level: High (80-100% RH)
Bulk PVB	2.6	2.8
Bare PVB Sample	1.5	1.6
PVB-Tedlar Sample	1.8	1.4
PVB-Foil Sample	1.7	1.9
Bulk EVA	2.0	2.1
Bare EVA Sample	2.1	2.2
EVA-Tedlar Sample	2.3	2.0
EVA-Foil Sample	2.3	2.2

resistance must have a much lower temperature coefficient. It is suspected to be the surface resistance of the PVB. Since the bulk resistance of EVA is three orders of magnitude higher than that of PVB, it is reasonable that the resistance properties of EVA samples are dominated by the bulk properties of the EVA, and not by its surface.

Sensitivity to Humidity. In analyzing the sensitivity to relative humidity it is useful to adopt an approach similar to the temperature-sensitivity analysis. Table 2 thus displays fraction leakage-current increase per 10% increase in relative humidity. Here it is seen that the PVB samples track the properties of the bulk PVB, except for the foil-covered sample, and the bare sample at high humidities. The partial sealing and long time constant for moisture sorption of the foil sample effectively damp out its humidity response.

Table 2. Humidity Sensitivity of Leakage Current (Factor Increase per 10% RH)

Sample Configuration	Humidity Level Low (30-50% RH)	Humidity Level High (80-100% RH)
Bulk PVB	1.9	1.6
Bare PVB Sample	1.9	2.5
PVB-Tedlar Sample	1.9	1.9
PVB-Foil Sample	1.3	1.5
Bulk EVA	1.3	1.1
Bare EVA Sample	1.9	1.1
EVA-Tedlar Sample	2.0	1.2
EVA-Foil Sample	1.5	1.1

In contrast, the humidity response of the EVA samples matches that of the bulk at high humidity levels and is significantly greater than the bulk at low humidity levels. This would seem to imply that the surface of the EVA may play an important resistive role at low relative humidities. Notice also that the low-humidity sensitivities of EVA and PVB samples are approximately equal (1.9 per 10% RH), and are approximately equal to the temperature sensitivity per 10°C. This adds credence to the practice of plotting reaction rate per (°C + % RH) as previously used by Otth and Ross (3).

Back-Cover Films. After having examined the general temperature and humidity sensitivities of the samples, it is useful to summarize the noted influence of the individual construction elements. From Figures 5 and 6, and Tables 1 and 2, it can be seen that the leakage-current performance of the EVA-Tedlar samples is essentially identical to that of the bare EVA samples. This observation can be explained by attributing similar bulk electrical conductivity and surface resistivity to EVA and Tedlar and recognizing that the thickness of the Tedlar (2 mils) is small relative to that of the EVA (18 mils).

Similarly, the leakage-current performance of the PVB-Tedlar samples is essentially the same as the bare PVB samples at low humidity levels (30 to 50% RH). However, at high humidity levels the Tedlar reduces the humidity sensitivity of the module to a value close to that of bulk PVB, and much less than that of the bare PVB sample. This leads to a factor of 3 to 5 reduction in leakage currents at the high humidity levels. The reduced current at high humidities is probably due to diminished dependence on a low PVB surface resistance, either due to the higher series resistance through the Tedlar, or due to a less humidity-sensitive surface on Tedlar.

Rear-Surface Foils. The addition of the Tedlar-Polyester-Aluminum-Tedlar (TPAT) to the rear surface of the samples has two effects: 1) it limits the sorption of water into and out of the encapsulant, and 2) it electrically shorts the surface of the sample, thus eliminating any dependence on surface resistivity. From the data in Figures 5 and 6, and Tables 1 and 2, it can be seen that the foil-film significantly reduced the humidity sensitivity from that of the non-foil samples, but led to leakage currents mid-way between the non-foil high- and low-humidity extremes. Because of the likely leakage of moisture into the edges of the foil samples, one should be cautious about reading too much into the foil-sample data. In the field the long sorption time-constant of a foil-backed module should totally isolate the encapsulant from diurnal humidity excursions, and result in some to-be-determined average humidity level. With the foil-film, the leakage current path is through the encapsulant thickness and Tedlar-polyester layers to the foil, thence across the foil to the module frame. The Tedlar-polyester layers should measurably increase the leakage resistance when used with high-conductivity encapsulants such as PVB, but play a secondary role with high-resistivity encapsulants such as EVA.

EVA Leakage Versus PVB Leakage. The bulk resistivity data displayed in Figure 1 suggest the leakage current in an unprotected PVB module should be three orders of magnitude greater than that of a similar EVA module. In fact the leakage current in the PVB samples was only greater by a factor of 15. This is an additional observation verifying the significance of the module-level factors affecting leakage currents and pointing again at the probable role of surface resistance.

Influence of Accrued Corrosion on Encapsulant Resistivity. One last positive finding was that extensive levels of accrued corrosion (on the order of 1 C/cm) had only a minor influence on the module insulation resistance. This is consistant with expectations and collaborates the practice of using beginning-of-life resistivity data (such as Figure 1) throughout a field-life simulation.

ANALYTICAL CONDUCTANCE MODELING

The above XTEST module leakage-current sensitivity study infers that corrosion rates are determined by a complex interplay of resistance paths including bulk, surface, and inter-material interfaces, each with differing temperature and humidity sensitivities. To shed some light on the interrelationship among these paths and to further interpret the XTEST findings, detailed 2-dimensional computer models of the conduction geometrics represented by the test modules were generated. Each model consisted of 200 to 300 nodes and was constructed using SINDA, which is a large general-purpose computer program with algorithms specifically developed to solve multi-dimensional conduction problems (8). The program outputs the voltage at each of the nodes together with the current flow between adjacent nodes.

The baseline model geometry, shown in Figure 7(a), was established to analyze the interplay between volume and surface resistivities as these parameters were varied relative to each other. Because of the complexity of the multi-hundred-node output, it is useful to visualize the results in terms of the simple lumped resistance model shown in Figure 7(b). The surface and bulk resistances R_s, R_a, R_b and R_d are schematic only and vary in complex ways as the surface resistivity (ρ_s) and bulk resistivity (ρ_v) are varied. The ultimate parameter determining the leakage current is the net resistance (R_T) from the cell to the frame, as determined by the series-parallel resistance network connecting the two. Figure 8 describes the manner in which R_T varies as the bulk and surface resistivities are varied, and as the key geometric parameters are varied. The numerical table at the top of Figure 8 indicates percentage distribution of leakage current between the surface (R_s) and bulk (R_d) paths, and the percentage voltage drop across each of the three resistors R_a, R_s, and R_b, in the surface path (see Fig. 7b). Examining these data provides insight as to which are the dominant resistance parameters and current paths for each region of the curve.

Far Left--Very Low Surface Resistance. When the surface resistance is negligible relative to the bulk resistance, the leakage current is controlled by resistances R_a and R_b in Figure 7(b). Under these conditions R_a and R_b are directly proportional to the thickness of the encapsulant (t) and inversely to the surface area of the cell and frame as determined by their widths (W and w). This is the case with a foil-covered module or when a module rear surface is shorted with liquid water (e.g., dew).

Central Region--Neither Resistance Dominates. When the surface and volume resistivities expressed in ohm and ohm-cm units are approximately equal, the voltage drop is distributed horizontally across the surface as well as through the

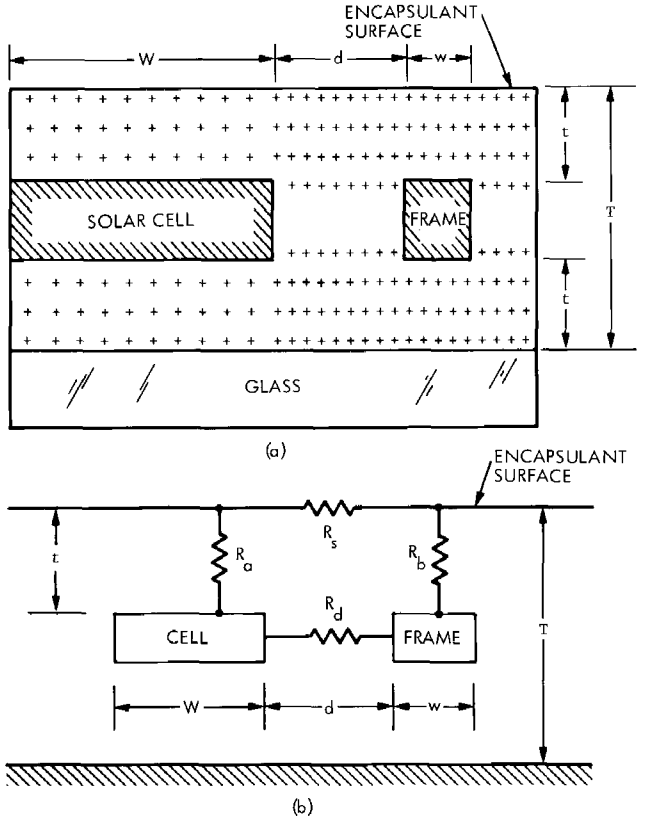

Figure 7. Electrical Conduction Models used to Analyze and Interpret Effects of Surface and Volume Resistivity

encapsulant thickness. The surface resistance is dominated by the surface resistivity integrated only across the gap spacing (d), and the encapsulant resistances (R_a and R_b) are associated with highly channeled currents emanating from the edges of the cell and frame adjacent to the gap. Because of this localized channeling, the resistance R_a is particularly sensitive to the thickness of the encapsulant right at the edge of the cell, an area where the encapsulant often thins as it flows to fill the cell-frame gap. Lateral conduction associated with R_d also begins to play a role as determined by the cell-frame gap. This central-region behavior is the phenomenon observed in the XTEST with bare-PVB samples; it may also apply to EVA modules when the surface is dry and resistive.

Far Right--Very High Surface Resistance. When the resistance of the surface approaches infinity, the conduction path is dominated by the lateral conduction (R_d) through the encapsulant; the gap spacing and total encapsulant thickness (T) are the determining parameters. This condition could exist when the surface is very clean and dry and the encapsulant is modestly conductive. Tedlar-covered PVB would be a possible example.

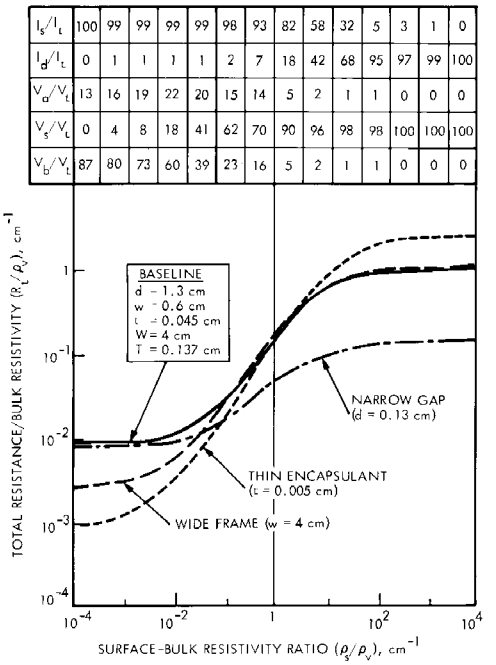

Figure 8. Sensitivity of Module Leakage Resistance to Encapsulant Surface-Bulk Resistivity Ratio

CONCLUSIONS

The analytical and experimental results summarized above illustrate the complexity of the electrochemical corrosion process and its dependency on many module and materials parameters. Temperature and humidity affect the various resistivity parameters by differing amounts and require that their influence be separately established for free-surfaces, material interfaces, and bulk encapsulants.

Although much of this characterization work is ongoing, a couple of important modeling, design, and test conclusions, can be drawn from the work to date.

(1) Leakage currents vary by orders of magnitude with modest changes in temperature and humidity, and the resulting changes in material resistivities may in turn cause the location of the dominant conduction paths to switch from surface to bulk and vice versa. This significant parameter sensitivity, together with the long time-constants required for equilibrium, suggest that extreme caution be exercized in the determination of acceleration factors for temperature-humidity tests and in the interpretation of leakage-current test results.

(2) When surface and bulk resistivities play equal roles (central region in Fig. 8), the leakage currents are very sensitive to surface resistance changes that could be caused by soiling, dew, etc. A conservative design might assume the surface shorted and select the encapsulant thickness (t) and resistivity (ρ_v) to maintain leakage currents at safe levels. The cell-frame gap should be chosen to provide a safety margin against edge delamination and intrusion (diffusion) of edge-sealant materials.

ACKNOWLEDGMENTS

The authors wish to acknowledge Professor John Orehotsky for obtaining the original encapsulant bulk conductivity data and the general assistance of Senior Engineering Assistant Elizabeth Jetter and technicians Scott Leland and Otto Witte.

REFERENCES

1. Mon, G., Orehotsky, J., Ross, R., Jr., and Whitla, G., "Predicting Electrochemical Breakdown in Terrestrial Photovoltaic Modules," Proceedings of the 17th IEEE Photovoltaic Specialists Conference, 1984, pp. 682-692.

2. Mon, G., Whitla, G., Ross, R., Jr., and Neff, M., "The Role of Electrical Insulation in Electrochemical Degradation of Terrestrial Photovoltaic Modules", IEEE Transactions on Electrical Insulation, December 1985.

3. Otth, D., and Ross, R.G., Jr., "Assessing Photovoltaic Module Degradation and Lifetime for Long Term Environmental Tests," Proceedings of the Institute of Environmental Science, 1983 Annual Technical Meeting, Los Angeles, California, April 19-21, 1983, pp. 121-126.

4. Gonzalez, C.C., Liang, R., and Ross, R.G. Jr., "Predicting Field Performance of Photovoltaic Modules from Accelerated Thermal and Ultraviolet Aging Data," Presented at the International Solar Energy Society Meeting in Montreal, Canada, June 22-29, 1985.

5. Martin, J.R., and Gardner, R.J., "Effect of Long Term Humid Aging on Plastics," Polymer Engineering and Science, V. 21, No. 9, June 1981, pp. 557-565.

6. Borman, W.F.H., "The Effect of Temperature and Humidity on the Long-Term Performance of Poly (Butylene Terephthalate) Compounds", V. 22, No. 14, October 1982, pp. 883-887.

7. Mon, G., and Ross, R.G., Jr., "Electrochemical Degradation of Amorphous-Silicon Photovoltaic Modules," Proceedings of the 18th IEEE Photovoltaic Specialists Conference, Las Vegas, Nevada, October 21-25, 1985.

8. Smith, J.P., SINDA User's Manual, Report No. 14690-H001-RO-00, Systems Group, TRW Co., 1971.